Direct calculation of k·p parameters for wurtzite AlN, GaN, and InN

D. J. Dugdale,* S. Brand, and R. A. Abram
Department of Physics, University of Durham, South Road, Durham DH1 3LE, United Kingdom
(Received 23 September 1999; revised manuscript received 16 December 1999)

Electronic band structure calculations have been performed for the wurtzite structures of AlN, GaN, and InN. In particular, the conventional $\mathbf{k}\cdot\mathbf{p}$ valence band parameters A_i $(i=1-7)$ have been computed from initial empirical pseudopotential calculations in two distinct ways. A Monte Carlo fitting of the $\mathbf{k}\cdot\mathbf{p}$ band structure to the pseudopotential data was used to produce one set. Another set was obtained directly from the formulas for the A_i in terms of the momentum matrix elements and energy eigenvalues at the center of the Brillouin zone. Both methods of calculating the $\mathbf{k}\cdot\mathbf{p}$ parameters produce band structures in excellent agreement with the original empirical band calculations near the center of the Brillouin zone. The advantage of the direct method is that it produces a unique set of $\mathbf{k}\cdot\mathbf{p}$ parameters, in contrast to a fitting procedure in which a range of equally valid parameter sets can exist.

I. INTRODUCTION

The semiconductors AlN, GaN, and InN and their ternary alloys have provoked great interest in the last few years. This interest is largely due to their optical properties, which offer numerous applications from full color displays to high density storage systems. Research over recent years has led to room temperature blue-violet laser emission in group III nitride quantum well structures for both pulsed[1,2] and continuous wave operation.[3]

The development of devices based on these materials has resulted in a demand for their characterization, and experimental and theoretical studies have established reliable values for such quantities as lattice parameters[4–6] and fundamental band gaps,[7–9] but many other parameters remain uncertain. For device modeling, calculations on optical gain have been performed on both bulk and quantum well structures.[10–12] In particular, the modeling of such devices requires band structure models, and much theoretical research has concentrated on providing these. Of these band structure models, the $\mathbf{k}\cdot\mathbf{p}$ method[13] using six or eight bands is one that is especially useful for device modeling. This is because the computational demands are light compared to other methods, such as those based on empirical pseudopotentials. The $\mathbf{k}\cdot\mathbf{p}$ approach is known to provide a good description of the heavy-hole, light-hole, and crystal field split-off bands at the zone center, which are important in any consideration of optical properties. Therefore, there is a need to obtain accurate $\mathbf{k}\cdot\mathbf{p}$ parameters for these wurtzite compounds and their alloys, in order to model current and future devices.

The parameters for $\mathbf{k}\cdot\mathbf{p}$ models must be determined from either experimental results or more fundamental calculations. Some existing work obtains these parameters indirectly, in that first the effective masses for electrons and holes at the Γ point are calculated using a parabolic line fit to existing band structure. Then, the $\mathbf{k}\cdot\mathbf{p}$ parameters are extracted from the effective masses using the relations that exist between them.[14] The parameters can also be obtained by fitting the $\mathbf{k}\cdot\mathbf{p}$ band structure to that of more sophisticated calculations, as in Refs. 15–17. In this paper we present a direct calculation of the $\mathbf{k}\cdot\mathbf{p}$ parameters and contrast it with a fitting approach. The motivation for this is to demonstrate the differences between the two methods and highlight the advantages of the direct calculation.

II. EMPIRICAL PSEUDOPOTENTIAL CALCULATIONS

The empirical psuedopotential calculations employed here use a local pseudopotential and a basis set consisting of approximately 60 plane waves per atom in the unit cell. Spin-orbit interactions are included using a simplified $K\times K'$ term (see, e.g., Ref. 18), which is adequate given the relatively small number of plane-waves employed in the calculation. In practice, our tests indicate that there are no appreciable differences between this scheme and the more sophisticated one adopted by, for example, Chelikowsky and Cohen.[19]

Pseudopotentials for each of the materials were generated using a procedure described in Ref. 20. These pseudopotentials were generated such that acceptable accuracy was achieved in several criteria, the foremost of which was the necessity to have good agreement with known band energies at the chosen symmetry points in the Brillouin zone. Secondly, it was required that there was good overall agreement between the predicted valence band structure and our own first-principles results obtained using VASP.[21–23]

III. k·p MODEL FOR THE WURTZITE STRUCTURE

We adopt a six band $\mathbf{k}\cdot\mathbf{p}$ model for the top of the valence band. Following Chuang and Chang,[24] the basis functions used are

$$|u_1\rangle=\frac{-1}{\sqrt{2}}|(X+iY)\uparrow\rangle,$$

$$|u_2\rangle=\frac{1}{\sqrt{2}}|(X-iY)\uparrow\rangle,\quad |u_3\rangle=|Z\uparrow\rangle,$$

$$|u_4\rangle=\frac{1}{\sqrt{2}}|(X-iY)\downarrow\rangle,$$

$$|u_5\rangle=\frac{-1}{\sqrt{2}}|(X+iY)\downarrow\rangle,\quad |u_6\rangle=|Z\downarrow\rangle, \tag{1}$$

where $|X\rangle$, $|Y\rangle$, and $|Z\rangle$ indicate the symmetry of the valence band zone center states, and the arrows represent the spin orientation. The z direction corresponds to the c axis of the wurtzite crystal.

The $\mathbf{k}\cdot\mathbf{p}$ Hamiltonian matrix in the basis defined by Eq. (3), where row/column i is associated with basis state $|u_i\rangle$, is

$$\begin{bmatrix} F & -K^* & -H_+^* & 0 & 0 & 0 \\ -K & G & H_- & 0 & 0 & \Delta \\ -H_+ & H_-^* & \lambda & 0 & \Delta & 0 \\ 0 & 0 & 0 & F & -K & H_- \\ 0 & 0 & \Delta & -K^* & G & -H_+^* \\ 0 & \Delta & 0 & H_-^* & -H_+ & \lambda \end{bmatrix}, \quad (2)$$

where

$$F=\Delta_1+\Delta_2+\lambda+\theta,$$

$$G=\Delta_1-\Delta_2+\lambda+\theta,$$

$$\lambda=\frac{\hbar^2}{2m_0}[A_1k_z^2+A_2(k_x^2+k_y^2)],$$

$$\theta=\frac{\hbar^2}{2m_0}[A_3k_z^2+A_4(k_x^2+k_y^2)],$$

$$K=\frac{\hbar^2}{2m_0}A_5(k_x+ik_y)^2,$$

$$H_+=\frac{\hbar^2}{2m_0}A_6(k_x+ik_y)k_z+iA_7(k_x+ik_y),$$

$$H_-=\frac{\hbar^2}{2m_0}A_6(k_x+ik_y)k_z-iA_7(k_x+ik_y),$$

$$\Delta=\sqrt{2}\Delta_3. \quad (3)$$

In the above expressions, $\Delta_1=\Delta_{cr}$, the crystal field splitting energy, and $\Delta_2=\Delta_3=\Delta_{so}/3$, where Δ_{so} is the spin-orbit splitting energy. The terms involving A_i $(i=1-6)$ arise from the contributions of remote bands which are calculated using Löwdin's perturbation theory.[25] These parameters are analogous to the Luttinger parameters used in the $\mathbf{k}\cdot\mathbf{p}$ models of zinc blende semiconductors. The Hamiltonian matrix above differs from that in Ref. 24 by the inclusion of terms linear in k, which involve the coefficient A_7 and are associated with the $\mathbf{k}\cdot\mathbf{p}$ term in the Hamiltonian.

The $\mathbf{k}\cdot\mathbf{p}$ parameters can be calculated by using the pseudopotential wave functions and energies at the zone center to evaluate the formulas for them. The Luttinger-like parameters can be expressed as:[24]

$$A_1=\frac{2m_0}{\hbar^2}L_2, \quad A_2=\frac{2m_0}{\hbar^2}M_3, \quad A_3=\frac{2m_0}{\hbar^2}(M_2-L_2),$$

$$A_4=\frac{2m_0}{\hbar^2}\left(\frac{L_1+M_1}{2}\right), \quad A_5=\frac{2m_0}{\hbar^2}\frac{N_1}{2}, \quad A_6=\frac{2m_0}{\hbar^2}\frac{N_2}{\sqrt{2}}, \quad (4)$$

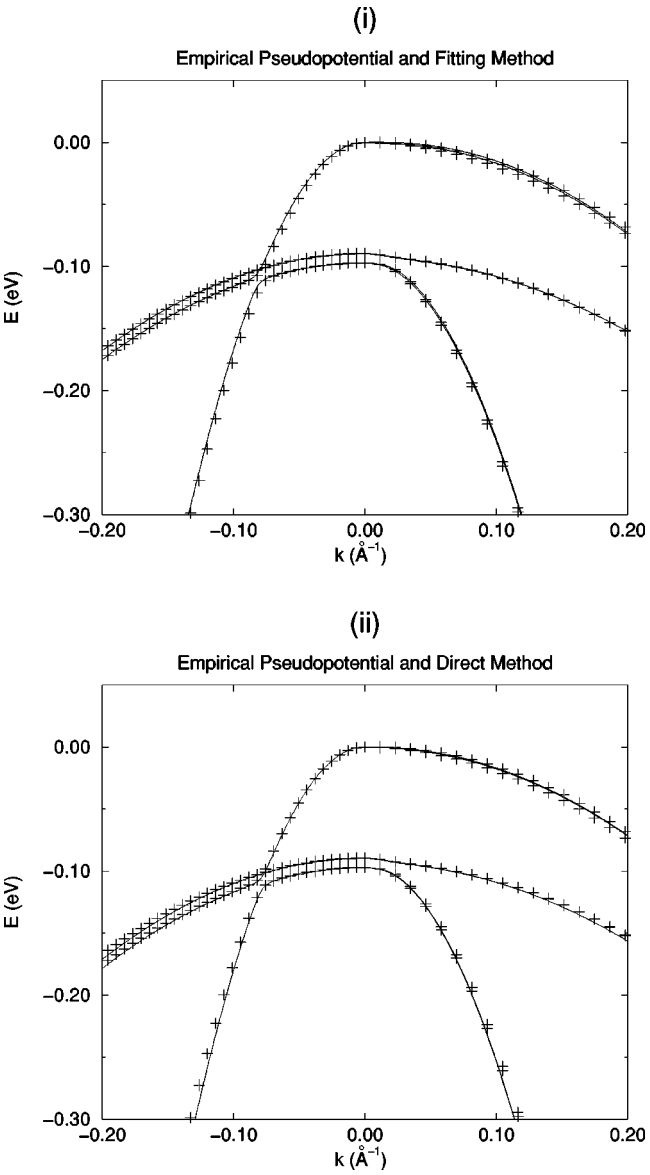

FIG. 1. Band structure close to the zone center (Γ point) for wurtzite AlN. The crosses represent the original band structure and the solid lines represent the $\mathbf{k}\cdot\mathbf{p}$ band structure. Negative k indicates a c axis (Γ-A) direction and positive k indicates an in-plane (Γ-M) direction. (i) and (ii) show the empirical pseudopotential band structure and the $\mathbf{k}\cdot\mathbf{p}$ band structures of the fitting method and direct method, respectively.

where

$$L_1=\frac{\hbar^2}{2m_0}\left(1+\sum_\gamma \frac{2p_{X\gamma}^x p_{\gamma X}^x}{m_0(E_0-E_\gamma)}\right), \quad (5)$$

$$L_2=\frac{\hbar^2}{2m_0}\left(1+\sum_\gamma \frac{2p_{Y\gamma}^y p_{\gamma Y}^y}{m_0(E_0-E_\gamma)}\right),$$

$$M_1=\frac{\hbar^2}{2m_0}\left(1+\sum_\gamma \frac{2p_{X\gamma}^y p_{\gamma X}^y}{m_0(E_0-E_\gamma)}\right),$$

$$M_2=\frac{\hbar^2}{2m_0}\left(1+\sum_\gamma \frac{2p_{X\gamma}^z p_{\gamma X}^z}{m_0(E_0-E_\gamma)}\right),$$

TABLE I. **k·p** parameters for wurtzite GaN. The A_i are in units of $\hbar^2/2m_0$, except A_7 where the units are eV Å.

	GaN							
	Present work		Ref. 14		Ref. 15		Ref.	Ref.
	Fit	Direct	Fit	Direct [a]	Fit	Quasicubic	16	17
A_1	−7.706	−7.979	−7.24	−7.17	−6.40	−6.36	−6.27	−6.40
A_2	−0.597	−0.581	−0.51	−0.44	−0.50	−0.51	−0.96	−0.80
A_3	7.030	7.291	6.73	6.64	5.90	5.85	5.70	5.93
A_4	−3.076	−3.289	−3.36	−3.62	−2.55	−2.92	−2.84	−1.96
A_5	−3.045	−3.243	−3.35	−3.57	−2.56	−2.60	−3.18	−2.32
A_6	−4.000	−4.281	−4.72	−4.04	−3.06	−3.21	−4.96	−3.02
A_7	0.194	0.179	−	−	0.204	0.000	<0.27	0.35
m_c^p (m_0)	0.15	0.15	0.17	0.17	0.23	0.19	0.20	0.18
m_c^z (m_0)	0.14	0.14	0.19	0.19	0.19	0.19	0.18	0.20
Δ_1 (meV)	22.3	22.3	21.0	21.0	36.0	−	73.0	24.0
Δ_2 (meV)	3.7	3.7	3.7	3.7	5.0	6.3	5.4	5.4
Δ_3 (meV)	3.7	3.7	3.7	3.7	5.9	6.3	5.4	6.8

[a]These are our directly calculated values using the empirical band structure parameters of Ref. 14.

$$M_3=\frac{\hbar^2}{2m_0}\left(1+\sum_\gamma \frac{2p^x_{Z\gamma}p^x_{\gamma Z}}{m_0(E_0-E_\gamma)}\right),$$

$$N_1=\frac{\hbar^2}{m_0^2}\sum_\gamma \frac{p^x_{X\gamma}p^y_{\gamma Y}+p^y_{X\gamma}p^x_{\gamma Y}}{m_0(E_0-E_\gamma)},$$

$$N_2=\frac{\hbar^2}{m_0^2}\sum_\gamma \frac{p^x_{X\gamma}p^z_{\gamma Z}+p^z_{X\gamma}p^x_{\gamma Z}}{m_0(E_0-E_\gamma)},$$

and $p^y_{X\gamma}=\langle X|p^y|\gamma\rangle$, $p^y=(\hbar/i)(\partial/\partial y)$.

The terms involving A_7 arise from matrix elements of the type $\langle X|k_x p^x|Z\rangle$ which result from the **k·p** term in the Hamiltonian rather than remote band effects. Such terms vanish by symmetry in the zinc blende but not the wurtzite structure. In much previous work the parameter A_7 has been assumed to be zero, but recently it has been shown that its inclusion can give an improved description of the valence bands.[26] The parameter A_7 can be evaluated using the formula

$$A_7=\frac{-i\hbar}{m_0\sqrt{2}}\langle X|p^x|Z\rangle. \tag{6}$$

Terms linear in k can also appear due to a linear k term in the spin-orbit interaction or through remote band effects of the spin-orbit interaction in association with the **k·p** term. These terms either vanish or are very small in zinc blende materials and are expected to be so here as well, particularly in view of the very small spin-orbit interaction in the nitrides. This view is confirmed by the results presented in Sec. V.

TABLE II. **k·p** parameters for wurtzite AlN and InN calculated from the fitting method and the direct method. The A_i are in units of $\hbar^2/2m_0$, except A_7 where the units are eV Å.

	AlN		InN	
Method	Fit	Direct	Fit	Direct
A_1	−4.367	−4.711	−9.470	−10.841
A_2	−0.518	−0.476	−0.641	−0.651
A_3	3.854	4.176	8.771	10.100
A_4	−1.549	−1.816	−4.332	−4.864
A_5	−1.680	−1.879	−4.264	−4.825
A_6	−2.103	−2.355	−5.546	−6.556
A_7	0.204	0.096	0.278	0.283
m_c^p (m_0)	0.25	0.25	0.10	0.10
m_c^z (m_0)	0.24	0.24	0.10	0.10
Δ_1 (meV)	−93.2	−93.2	37.3	37.3
Δ_2 (meV)	3.7	3.7	3.7	3.7

IV. CALCULATION OF THE k·p PARAMETERS

Two methods have been used to obtain the parameters for the **k·p** model. In the first method, the values of the A_i were obtained through a simple Monte Carlo fitting procedure to the band structure. The empirical pseudopotential method was used to calculate the band structure at several k points over the range shown in Fig. 1. The **k·p** method was then used to calculate the band structure at these same k points, using a set of A_i values. These A_i values were then varied using a Monte Carlo technique, and the process systematically repeated until the **k·p** eigenvalues were in good agreement with those of the empirical pseudopotential calculations. In this approach each of the sampling points was given a weight, with those closer to the zone center typically being weighted more than those further away. Additionally, the bands themselves were also appropriately weighted.

In the second method, the **k·p** parameters were evaluated directly from Eqs. (4)–(6). To obtain these parameters, 250 bands are included in each summation in Eq. (5). These sums are rapidly convergent, with all of the **k·p** parameters converged to within 1% of their final value after a summation

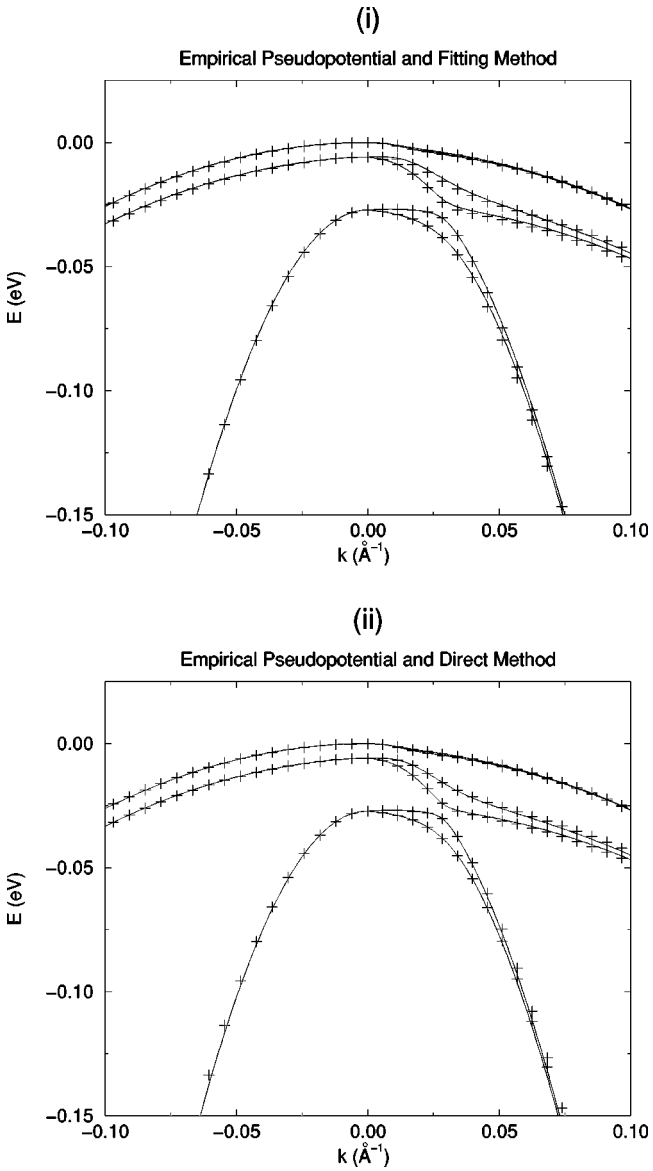

FIG. 2. Band structure close to the zone center for wurtzite GaN. See Fig. 1 for an explanation of the notation.

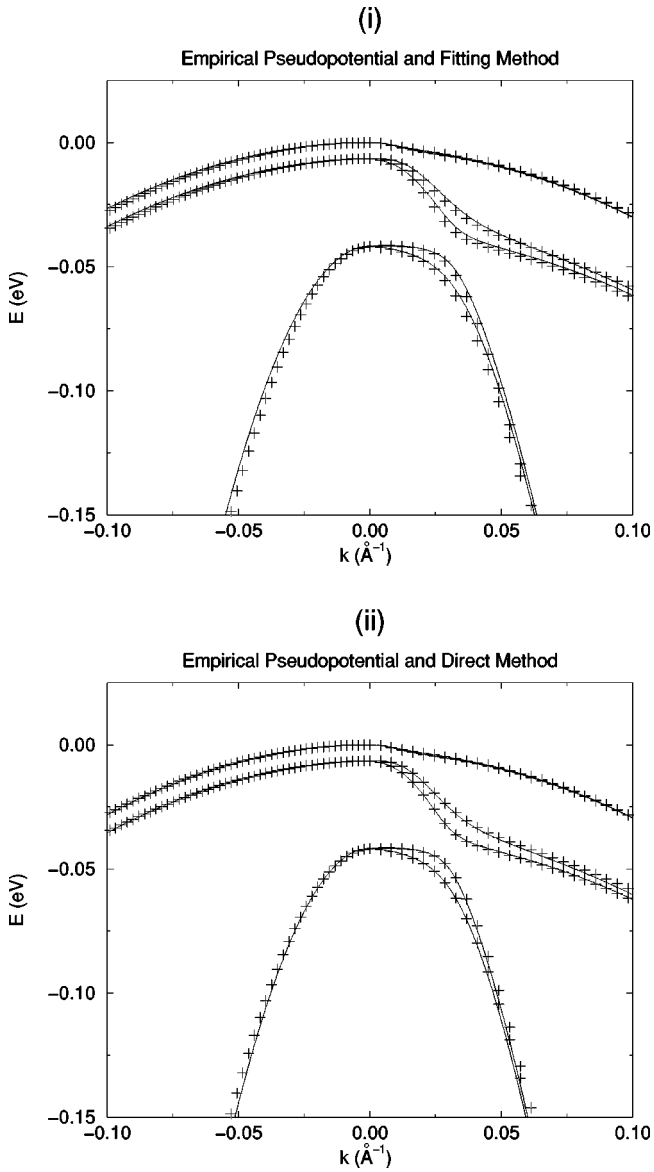

FIG. 3. Band structure close to the zone center for wurtzite InN. See Fig. 1 for an explanation of the notation.

over just 60 bands, and thus the parameters obtained using this method are unique for a given empirical band structure.

V. RESULTS

The calculated values of A_i $(i=1-7)$ for GaN, together with those from other calculations, are presented in Table I. The values for AlN and InN obtained in this work are shown in Table II. The parameters from the two different methods were used in $\mathbf{k}\cdot\mathbf{p}$ calculations of the band structures of GaN, AlN, and InN in the region of interest close to the Γ point. The resulting band structures are shown in Figs. 1–3. Note that AlN has a negative crystal field splitting, and thus the ordering of the bands is different from that of GaN and InN. For all three materials, both the Monte Carlo fitting approach and the direct method produced band structures in very good agreement with those of the original empirical pseudopotential calculation. In particular, the inclusion of A_7 accurately models the lifting of the degeneracy near the anticrossing feature seen in GaN and InN. Also, note that these bands are extremely nonparabolic, and thus obtaining effective masses (and subsequently $\mathbf{k}\cdot\mathbf{p}$ parameters) from them via parabolic line fits is not preferable to the methods presented here.

From Tables I and II, it is clear that our parameters obtained by Monte Carlo fitting and the direct approach are somewhat different from each other for each of the materials. For AlN, the difference in the A_i values is typically about 10%. For GaN, the agreement is better, with differences at around 6%, and for InN the values generally differ by about 13%. However, despite these differences, both methods give a very similar quality of fit to the original band structure, as can be concluded from the results shown in Figs. 1–3. This demonstrates the potential inconsistency of the fitting method, in that two different sets of parameters appear to result in equally good agreement with the initial band structure. Indeed, for the fitting procedure a range of equally valid parameter sets exists, and it is because of this that it cannot be relied upon to give consistent $\mathbf{k}\cdot\mathbf{p}$ parameters for a series of alloy compositions. In contrast to the fitting approach, the

method of obtaining **k·p** parameters directly from the zone center wave functions and energies has a firm physical basis and presents an unambiguous route to calculating these quantities from a given original band structure. Consequently, this method can be applied to a series of alloy compositions, with the expectation that consistent **k·p** parameters will be obtained.

In addition to our own results, Table I also shows the **k·p** parameters that have been reported in the literature by other workers. Our results are most similar to those of Yeo *et al.*,[14] who also employ an empirical pseudopotential method. We have additionally calculated A_i $(i=1-6)$ directly using the empirical band structure of Yeo *et al.* The agreement between this new set and that originally obtained by Yeo *et al.* is fairly good. The other values quoted in Table I are based on first-principles calculations, and while they are qualitatively similar to our own results the individual A_i parameters can significantly differ. This is to be expected given that our empirical band structure is quite different from the first-principles band structures used in the fittings for these results.

Our values in Tables I and II can also be considered with respect to the cubic approximation to the wurtzite structure.[16,27] This approximation is based on the similarity between the zinc blende and wurtzite structures, in that they are both tetrahedrally bonded but with different stacking arrangements. For the cubic approximation, the following relations can be established between the Luttinger-like parameters:

$$A_1 = A_2 + 2A_4,$$

$$A_3 = -2A_4,$$

$$A_3 + 4A_5 = \sqrt{2}A_6. \tag{7}$$

Although there is no requirement for these relationships to be satisfied in our calculations, we note that substitution of the values of Tables I and II in Eq. (7) shows that the cubic approximation is satisfied approximately. For AlN, comparing the actual value on the left hand side of Eq. (7) with the value determined by the right hand side, the relations are satisfied to within 20% for the fitting method and to within 13% for the direct method. For GaN, the values are within 13% for the fitting method and 10% for the direct method. For InN, the approximation holds somewhat better, with values for both methods within about 5% of those predicted.

VI. CONCLUSIONS

Two methods have been presented to obtain **k·p** parameters from existing empirical pseudopotential band structures in wurtzite semiconductors. Obtaining the parameters using a Monte Carlo fitting approach gives **k·p** band structures in excellent agreement with the original empirical band structures. The direct technique employed to obtain these parameters also produces excellent band structure near the center of the Brillouin zone, and has the advantage of producing a unique set for a given empirical band structure. Given that this method has a sound theoretical basis, and produces **k·p** band structures of comparable quality, we consider it to be preferable to an arbitrary fitting procedure. It has the particular advantage of being able to produce consistent sets of parameters for studies such as those involving a series of alloy compositions.

We have therefore constructed sets of **k·p** parameters for wurtzite AlN, GaN, and InN. These results serve as a basis for further work on the electronic structure of alloys of varying compositions for calculations of optical properties and device modeling.

ACKNOWLEDGMENTS

The authors are grateful to EPSRC for funding this research through a research grant and the provision of financial support for D.J.D. We also thank Dr. R. A. Coles for useful discussions.

*Electronic address: D.J.Dugdale@durham.ac.uk

[1] I. Akasaki, H. Amano, S. Sota, H. Sakai, T. Tanaka, and M. Kaike, Jpn. J. Appl. Phys., Part 2 **34**, L1517 (1995).

[2] S. Nakamura, M. Senoh, S. Nagahama, N. Iwasa, T. Yamada, T. Matsushita, H. Kiyoku, and Y. Sugimoto, Jpn. J. Appl. Phys., Part 2 **35**, L74 (1996).

[3] S. Nakamura, M. Senoh, S. Nagahama, N. Iwasa, T. Yamada, T. Matsushita, Y. Sugimoto, and H. Kiyoku, Appl. Phys. Lett. **70**, 868 (1997).

[4] H. Schulz and K. H. Thiemann, Solid State Commun. **23**, 815 (1997).

[5] A. F. Wright and J. S. Nelson, Phys. Rev. B **51**, 7866 (1995).

[6] I. Gorczyca and N. E. Christensen, Physica B **185**, 410 (1993).

[7] T. Lei, M. Fanciulli, R. J. Molnar, T. D. Moustakas, R. J. Graham, and J. Scanlon, Appl. Phys. Lett. **95**, 944 (1991).

[8] *Numerical Data and Functional Relationships in Science and Technology*, edited by K. H. Hellwege, Landolt-Börnstein, New Series, Group III, Vol. 17, pt. a (Springer, New York, 1982).

[9] R. Dingle, D. D. Sell, S. E. Stokowski, and M. Ilegems, Phys. Rev. B **4**, 1211 (1971).

[10] M. Suzuki and T. Uenoyama, Appl. Phys. Lett. **69**, 3378 (1996).

[11] J. B. Jeon, B. C. Lee, Y. M. Sirenko, K. W. Kim, and M. A. Littlejohn, J. Appl. Phys. **82**, 386 (1997).

[12] Y. C. Yeo, T. C. Chong, M. F. Li, and W. J. Fan, J. Appl. Phys. **84**, 1813 (1998).

[13] E. O. Kane, J. Phys. Chem. Solids **1**, 82 (1956).

[14] Y. C. Yeo, T. C. Chong, and M. F. Li, J. Appl. Phys. **83**, 1429 (1997).

[15] K. Kim, W. R. L. Lambrecht, B. Segall, and M. Schilfgaarde, Phys. Rev. B **56**, 7363 (1997).

[16] M. Suzuki, T. Uenoyama, and A. Yanase, Phys. Rev. B **52**, 8132 (1995).

[17] J. A. Majewski, M. Sta''dele and P. Vogl, in *III-V Nitrides*, edited by F. A. Ponce, T. D. Moustakas, I. Akasaki, and B. A. Monemar, MRS Symposia Proceedings No. 449 (Materials Research Society, Pittsburgh, 1997), p. 887.

[18] M. L. Cohen and V. Heine, Solid State Phys. **24**, 73 (1970).

[19] J. R. Chelikowsky and M. L. Cohen, Phys. Rev. B **14**, 556 (1976).

[20] S. K. Pugh, D. J. Dugdale, S. Brand, and R. A. Abram, Semicond. Sci. Technol. **14**, 23 (1999).

[21] G. Kresse and J. Hafner, Phys. Rev. B **47**, 558 (1993).
[22] G. Kresse and J. Furthmüller, Comput. Mater. Sci. **6**, 15 (1996).
[23] G. Kresse and J. Furthmüller, Phys. Rev. B **54**, 11 169 (1996).
[24] S. L. Chuang and C. S. Chang, Phys. Rev. B **54**, 2491 (1996).
[25] P. O. Löwdin, J. Chem. Phys. **19**, 1396 (1951).
[26] G. B. Ren, Y. M. Liu, and P. Blood, Appl. Phys. Lett. **74**, 1117 (1999).
[27] G. L. Bir and G. E. Pikus, *Symmetry and Strain-Induced Effects in Semiconductors* (John Wiley and Sons, New York, 1974).